Dynamic, LiDAR-based assessment of lighting conditions in Pacific Northwest forests

Demetrios Gatziolis[1]

USDA Forest Service, PNW Research Station, e-mail:dgatziolis@fs.fed.us

Paper Number: SL2012-170

Abstract: Light Detection and Ranging (LiDAR) technologies employed over forested landscapes provide a detailed representation of dominant objects, typically tree crowns and ground surfaces. In this study, the actual lighting regime within a forest stand is derived from LiDAR data in a two-stage process. First, a LiDAR data-derived ground surface raster is used to determine whether physiographic conditions around the targeted area affect direct sun illumination. The second stage operates on the voxel domain, which partitions space in discrete cubical elements and labels them either filled, if they contain at least one laser return, or empty otherwise. A buffer around the area of interest ensures that shadowing induced by surrounding vegetation is considered in the computations. Ray tracing through the voxel space along the trajectory that connects the sun and each facet of each filled voxel classifies the facets as either sunlit or in shadow. The process can be repeated for additional sun locations or time intervals from sunrise to sunset for a given day. Ultimately, the daily cumulative or time-interval-specific amount of direct sunlight during a cloudless day can be computed. Adequate hardware resources are critical for reasonable computing times over large areas or fine time intervals. The methodology described above was evaluated using precisely georeferenced and timed field observations of ground illumination conditions in forest stands in eastern Oregon. Remarkable agreement between recorded and derived lighting conditions was observed. This methodology for computing lighting regime wherever high-density LiDAR data are available has various potential applications including contributions to forest growth and yield models, assessment of regeneration potential, stream shading, and in support of management and tactical decision making.

1. Introduction

Sunlight is a major environmental and ecological factor. Within forest stands, sunlight, or simply light, availability is affected by the amount and spatial distribution of above-ground vegetation (Parent and Messier, 1996), topography, and by diurnal and seasonal cycles in the sun trajectory. Light availability is known to limit the survival and growth of many forest species (Comeau *et al.* 1993; Nicotra *et al*. 1999), and to affect agroforestry system practices (Bellow and Nair 2003), the dispersal of invasive species (Parendes and Jones, 2000), stream temperature (Chen *et al*. 1998), and many other phenomena and activities. Considering the high variability of light availability in space and time observed in field conditions, the explicit, distributed assessment of light conditions is regarded as an ill-posed task primarily due to the tremendous, and seldom met data requirements on the structural elements of a forest stand (Brunner, 1998). To overcome these limitations, various simplifying assumptions are made concerning the main structural elements of a forest stand, and light availability is assessed via modeling (e.g. MacFarlane *et al*. 2003). Tree crowns in the models are represented by simple geometrical shapes such as cones, cylinders, or ellipsoids. Model predictions routinely serve as input to growth and yield models or in support of forest management decisions. Field measurements of instantaneous light availability necessary for model development are typically obtained by processing hemispherical photos, or by using quantum sensors during overcast conditions. All options add substantial logistical cost to an already complex effort.

Accurate assessment of temporal sun illumination regimes within forests might be attainable where Light Detection and Ranging (LiDAR) data are available. Assuming adequate density in the return point cloud, renditions of the LiDAR data in three-dimensions (3D) presented to humans are perceived as detailed representations of tree crowns and of the ground, the dominant structures in a forested scene. If LiDAR data could be consistently converted to a 3D representation of vegetation objects, the interaction between these objects and the light emitted from a source positioned somewhere within or outside the scene could be calculated analytically. A simplified variant of this approach is emerging with increasing frequency in forest applications. It involves a highest-return raster surface generated from the LiDAR data that is processed with an implementation of the hillshade algorithm (eg. Burrough and McDonell, 1998) for a specified sun azimuth and elevation angles to determine the sunlit cells and those in shadow. While this approach might be a useful approximation of lighting regimes when the sun is at a high elevation angle, unfortunately it is biased and favors cells in shadow. The bias is introduced primarily by the consistent exaggeration of the volume occupied by tree crowns and also by the inability of the raster representation, sometimes known as a 2.5D rendering, to consider illumination of vegetation and ground portions that are overtopped by vegetation. This study introduces an alternative approach potentially capable of providing accurate illumination estimates. Its performance is evaluated using actual light availability observations in eastern Oregon.

2. Methods

Voxel-based modeled and LiDAR-based representations of ground surfaces and vegetation are intersected, or traversed, by rays that mimic solar illumination. A series of simulations for different sun positions are performed and the resulting illumination regimes are summarized.

2.1 Study area and field data

The approximately 190,000 ha study area is located in the Malheur National Forest in eastern Oregon, USA, where elevation ranges from 1,250 to 2,600 m (Figure 1a). Dominant species include Ponderosa pine (*Pinus ponderosa*), Douglas-fir (*Pseudotsuga menziesii*), western larch (*Larix occidentalis*), grand fir (*Abies grandis*), and lodgepole pine (*Pinus contorta*). The Forest exhibits a variety of physiographic conditions and the majority of forest stands feature open canopies with medium, between 30 and 60 percent, canopy cover. The study area contains 186 Forest Inventory and Analysis (FIA) Program plots with more than 5,000 tallied trees. FIA uses

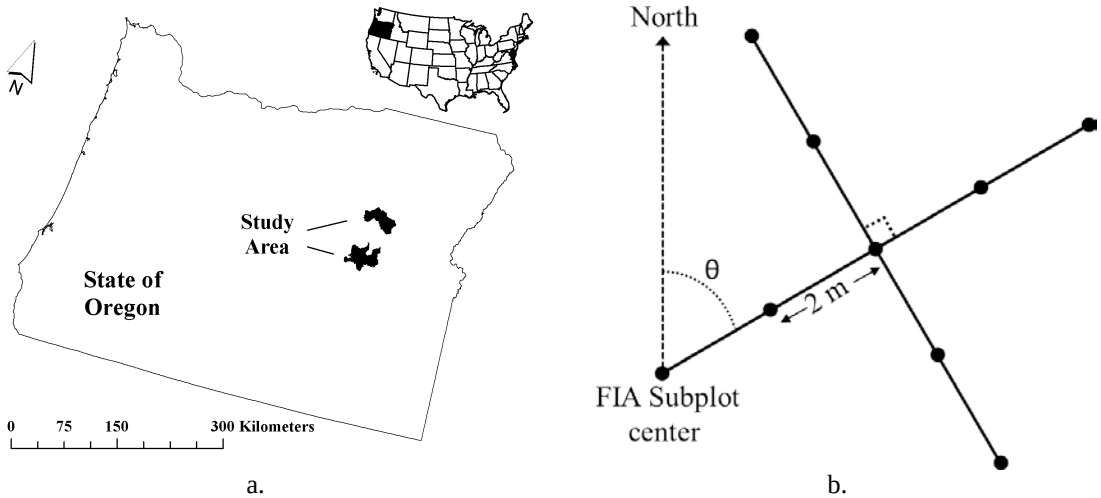

a. b.

Figure 1: a. Study area in the Malheur National Forest, and b. Field protocol for solar illumination observations

a clustered design with each plot comprising 4 subplots. Solar illumination conditions were recorded in 54 FIA subplots in the summer of 2010. Randomly oriented transects were established in each subplot arranged as shown in Figure 1b and illumination conditions were recorded at two meter intervals from the edge of each transect. Each observation was timed and assigned a code; 0 if in shadow, 2 if sunlit, and 1 if very close to the boundary between sunlit and shadowed areas. An index value, computed as the mean of all observations per subplot, quantified the solar illumination conditions. Coordinates of submeter precision were obtained at each subplot center via post-processed differential Global Positioning System data.

2.2 LiDAR data

Discrete return, airborne LiDAR data were acquired over the study area in 2008 and 2009 with two instruments; a Leica ALS50 Phase II and a Leica ALS60. Both operated with pulse frequency of 105 kHz and are capable of recording up to 4 returns per pulse. An average 55 percent scanning swath sidelap, mean instrument-target range of 920 m, mirror scan frequency of 52, and return filtering to a maximum scan angle of 14 degrees yielded a mean density of 9 returns per square meter. The nominal footprint diameter and spacing were 28 and 68 cm respectively. A 0.91-m, LiDAR-derived Digital Terrain Model (DTM), was provided by the data vendor.

2.3 Modeled and LiDAR-based voxel scene representation

By using tree size information recorded during field visits of FIA plots, species-specific crown shape templates, and Forest Vegetation Simulator (Shaw 2009) formulae which estimate tree crown radius from stem diameter at breast height, 3D crown and stem models were generated for each tallied tree. The distribution of plot tree density was also assessed. Crown shape templates were designed as weighted combinations between cones and ellipsoids of predefined eccentricity. Stems were depicted as cones (Figure 2a). One hundred realizations of modeled tree stands, henceforth referred to as scenes, each 4 hectares in size, were then generated by sampling from the plot tree density distribution and the list of reconstructed crown shapes from the tallied trees (Figure 2b). The spatial distribution of stems in the modeled stands followed a Strauss (1975) process, a compromise between a regular point pattern (on a grid) and a complete random one. A Strauss point pattern is believed to approximate the spatial arrangement of trees in the Malheur National Forest. The geometric shapes of tree crowns and stems in the scene were then converted to a voxel representation. The latter is defined as the partitioning of space into discrete cubic elements. Voxels with center within a modeled stem or crown were labeled ‘filled’ otherwise they were labeled ‘empty’. Terrain in all modeled scenes was considered flat.

The 4-ha, LiDAR-based scene representations were centered on each of the 54 subplots. The buffer area around each subplot center ensures that the influence on illumination conditions of both the surrounding vegetation and the local topography is considered. Voxels containing one or more above-ground returns were labeled filled. Returns with above-ground elevation below 1 m were excluded from the voxel labeling process to ensure a clear distinction between ground and vegetation voxels. The former were identified using the DTM provided by the data vendor.

2.4 Voxel traversal by sun rays

Prior to actual voxel traversal operations, the illumination of cells in the subplot DTM is examined by application of the hillshade algorithm for all desired sun locations. Pronounced geomorphological features in the vicinity of the subplot such as mountain peaks, ridges, or steep

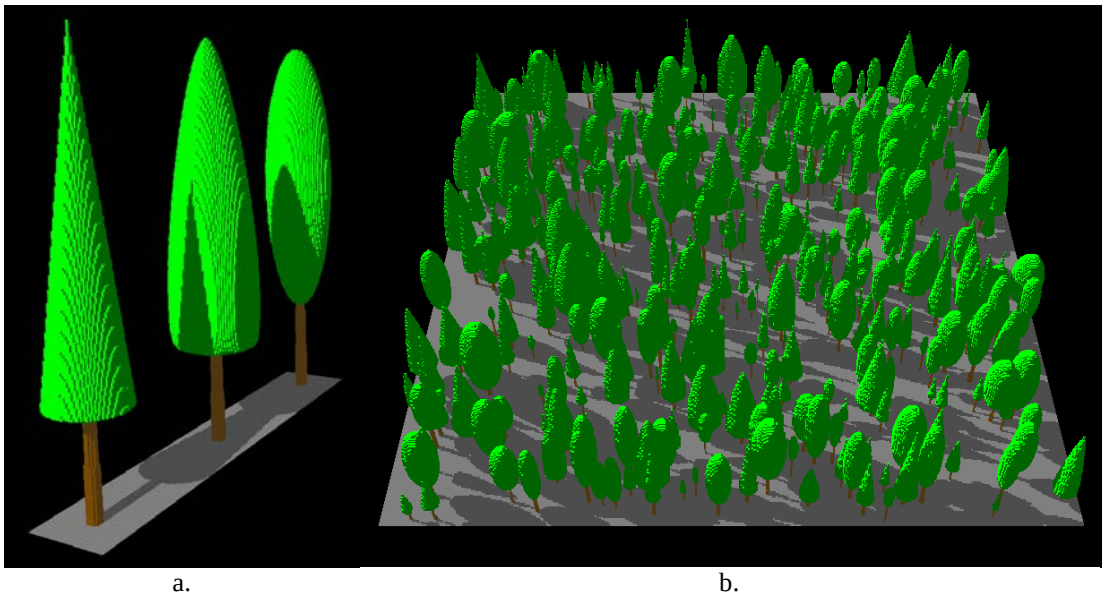

a. b.

Figure 2, a. Perspective view of modeled trees with, from front to back, conical, weighted and ellipsoidal crown shape; and b. Perspective view of modeled, 4-ha scene.

terrain could block incoming solar rays and if their presence is not considered sunlit conditions will be overestimated. After the absence of topography-induced shading effects has been confirmed, the directional vectors of the sun rays to the center of the parallelepiped enveloping the scene voxels are computed. The directional vectors are assumed constant within the scene considering its size in relation to the distance to the sun.

The voxel traversal by sun rays is a modification of the method by Amanatides and Woo (1987). For a given sun location, rays are generated towards the center of every visible voxel facet (side) in the scene. For each ray, the directional vectors calculated for the current sun location are used to determine the coordinates of the entry point to the scene. As the ray progresses towards the targeted voxel facet, its intersections with other voxel facets are computed and the label of the each voxel is examined. The ray terminates if it intersects the facet of a filled voxel. A facet is labeled sunlit only if it is reached by the ray directed to its center. The entire process, including the construction of the modeled scenes, was scripted in the C programming language with multithreading support. Sun azimuth and elevation angles for specific locations and times were computed by using a library compiled by Reda and Andreas (2008).

2.5. The role of voxel resolution

It was determined via experimentation with modeled scenes that, for a given solar position, as resolution becomes coarser, scene surfaces in shadow increase at the expense of those sunlit. The voxel resolution and sunlit or shadowed area relationship was found to be linear, and the underestimation of sunlit areas for a given resolution was more pronounced where tree density was higher (Figure 3a). This observation from the modeled scenes implies that unbiased assessment of light conditions via voxel representations, at least for crowns modeled as concave objects with continuous surfaces, is possible only with very fine voxel resolution. If applied to LiDAR-derived scenes, such a constraint would undermine the entire approach because, with too fine a resolution voxels, the representations of crowns would be exceedingly sparse even for high-density acquisitions. Hence, the sunlit areas would be grossly overestimated. Conversely, if resolution is too coarse, the volume occupied by crowns would be inflated and lead to overestimation of shadows. Thankfully, however, it was subsequently determined that consistently accurate estimates can be obtained even with coarser voxel resolutions. This was

accomplished by directing, instead of one, four sun rays towards each visible voxel facets in the arrangement seen in the inset of Figure 3b, and by labeling the facet sunlit as long as at least one ray were to reach it (Figure 3b). The four-ray per facet option was employed for all LiDAR-derived scenes.

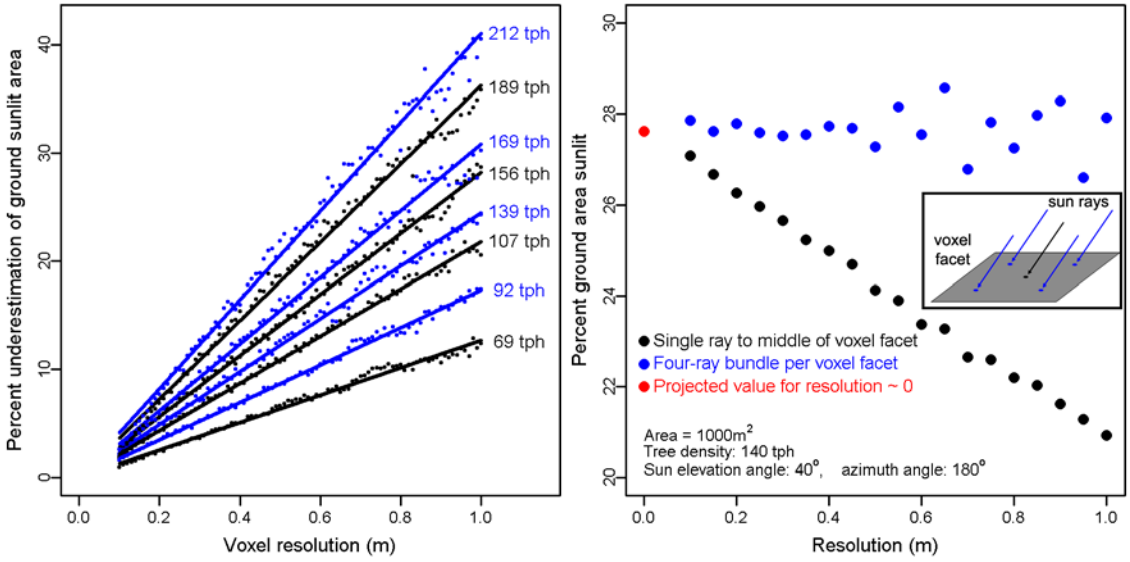

a. b.

Figure 3, a. Relationship between voxel resolution and extent of sunlit areas in modeled stands as function of tree density, and b. effect of sun ray density and distribution [inset] on sunlit conditions.

Determining the resolution that yields accurate estimates of solar illumination regimes is therefore critical and dependent on the local density of the return cloud. Since return density seldom is stationary across the acquisition area, the optimal voxel resolution has to be determined dynamically. Following experimentation with independent field observation of light availability, the optimal voxel resolution was determined as the mean local spacing in tow dimensions among above-ground returns with elevation value within 2 m from the highest-return raster surface.

3. Results and Discussion

The resolution of the LiDAR data-derived voxel scenes centered on each of the 54 subplots with light observations ranged from 53 to 69 cm (mean 59 cm). The volume occupied by voxels containing at least one return from subplot tree crowns ranged between 25 and 65 percent of the volume that would have been occupied if the crowns of those trees had been modeled using the procedure described in section 2.3. Lower and internal crown components exhibited sparser representation.

Despite the voxel density and continuity issues for most crowns, a remarkable agreement between LiDAR-derived and field-measured sunlit illumination of ground surfaces was observed (Figure 4). The slope of field-measured values regressed linearly against the LiDAR-derived ones was not different from 1 at $\alpha = 0.01$. This finding indicates that the methodology employed is capable of delivering unbiased estimates of solar illumination regimes, at least in the presence of vegetation and LiDAR return density conditions similar to those evaluated in this study. Of the two outliers observed, the first with field index value approximately 0.5, or 25% direct sunlit illumination, belonged to an area with noted budworm infestation. In the year

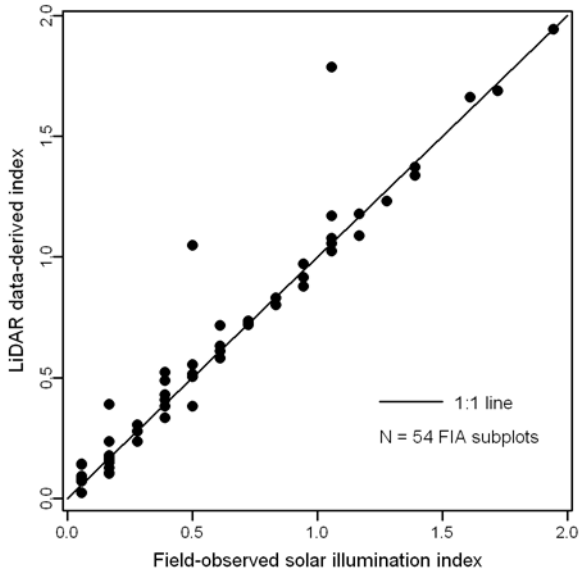

Figure 4, Comparison of LiDAR-derived estimates and field observations of ground solar illumination.

elapsed between LiDAR data acquisition and field light measurements, progression in infestation intensity and ensuing reductions in crown foliage could be responsible for overestimation of sunlit conditions. The second outlier was a subplot positioned at the edge of a forest stand towards a sizeable opening, where instability in aircraft attitude resulted in return density much lower than the mean across the entire acquisition. The ensuing undersampling of crowns at the edge of the stand likely led to overestimation of the light regime.

Visual qualitative assessment of LiDAR return clouds or even voxel representations suggests that ocular estimates of sun light illumination conditions can be substantially overestimated. In the scene shown in Figure 5 (a. and b.), only about 10 percent of the ground at the central half area of the scene is actually sunlit, an amount much less than the mean of 30 percent suggested by human cognition for the mid-morning of a summer day. Figure 5c illustrates the importance of using a buffer around the area of interest to negate scene edge effects. It was found that increasing the buffer width beyond 1.5 times the mean tree height did not improve the accuracy of sunlit area estimates. Cumulative estimates of sunlit conditions for a day (Figure 5d), or longer period, exhibited substantial variability and pronounced local spatial continuity.

The key concept of this study is the assumption that representations of tree crowns generated from LiDAR return clouds support analytical and explicit calculations regarding the timing and duration of solar illumination conditions within forest stands. With most recent LiDAR acquisitions in the State of Oregon obtained in high density and extending over large areas, the utility of dynamic light availability estimates evolves from a theoretical exercise to a practical management and decision making tool. The transition from concept to implementation required decisions on often elusive components that are integral to the implementation procedure such as the voxel resolution appropriate for each scene and number of rays to use. By using modeled representations of tree crowns, the effects of these components on the illumination estimates could be investigated, quantified, and ultimately controlled thereby ensuring estimation accuracy. Emphasis was given to multithreaded computational support which early on emerged as a logistical prerequisite, considering that each scene explored comprised over 7 million voxels, and the need to repeat the computations for series of solar positions.

The very good agreement between LiDAR-derived and field-recorded sun light conditions may not necessarily hold when the sun is low above the horizon. At low solar elevation angles, many

sun ray trajectories intersect exclusively the lower portions of crowns where the density of filled voxels is reduced. Since all field data were obtained within 4 hours from solar noon, the performance of this method could not be determined for early morning or pre-dusk times.

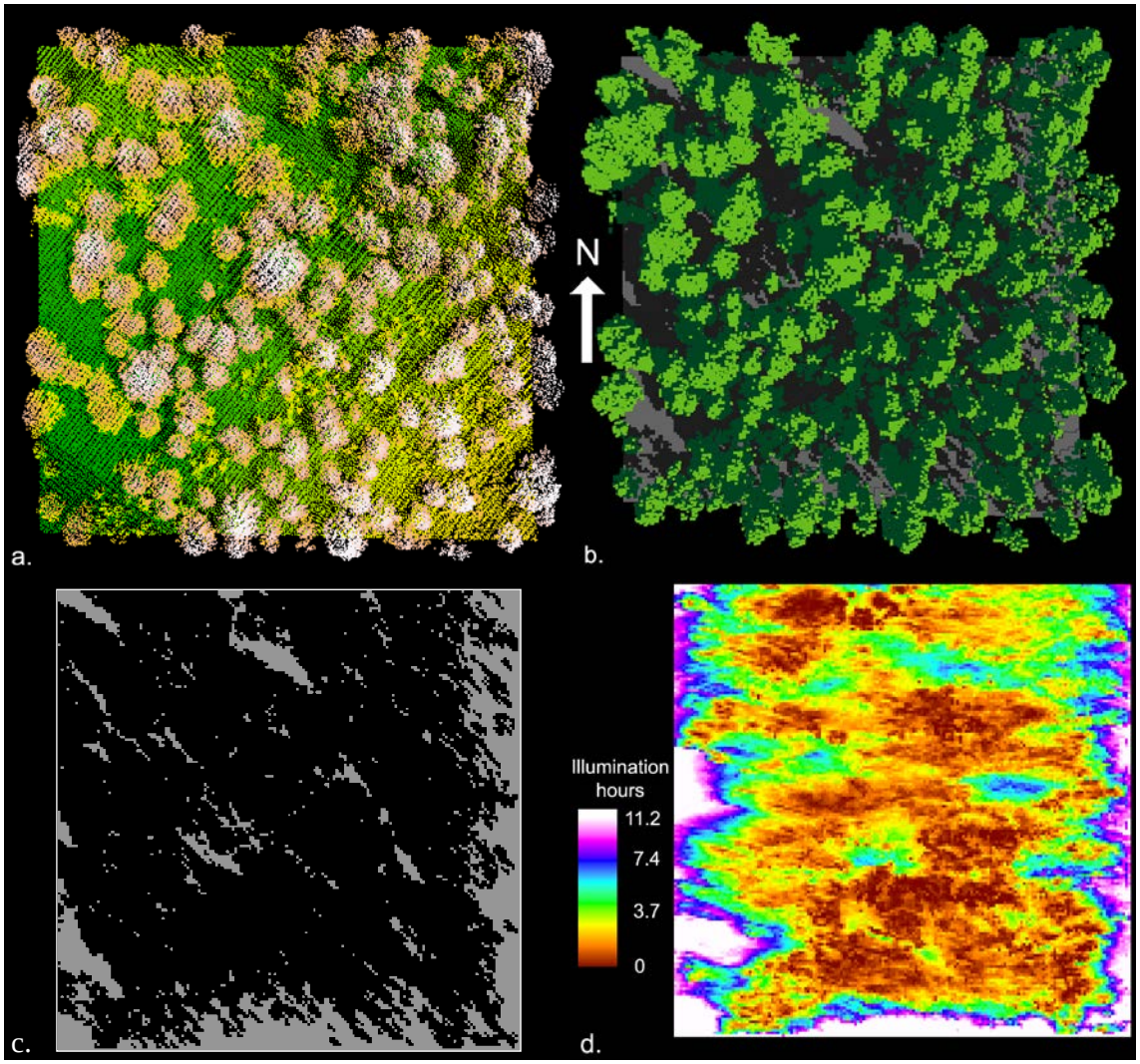

Figure 5, a. Nadir view of return point cloud, with light colors representing higher return elevation; b. corresponding nadir view of morning solar illumination conditions calculated and shown in voxel space; c. ground illumination conditions as in (b) but with vegetation not shown and light/dark tones representing sunlit/in shadow voxels respectively; and d. mean sunlit index of ground voxels for a mid-summer,12-hour period centered on solar noon.

At its present development stage, the traversal of LiDAR data-derived voxel scenes considers only direct sunlight, and tree crowns are assumed to be opaque objects. As it can be seen in Figure 2a, the shadow of modeled crowns cast on the ground or on adjacent crowns contains no sunlit portions. The suggested approach for dynamically determining the optimal voxel resolution of the LiDAR-derived scenes also aims at generating opaque crowns without any, or with minimal openings within them. Since light transmittance through the canopies is not yet considered, all sunlit indices calculated lack the diffuse solar illumination component. This limitation, however, can likely be addressed by directing towards each visible facet a predefined distribution of regularly spaced rays in a hemispherical arrangement. The ratio of rays that reach the facet to the total would quantify scene openness around the facet and serve as surrogate of diffuse lighting conditions. Considering that scene openness is not subject to

diurnal cycles, the computation load for obtaining both direct and diffuse sunlight illumination conditions could be manageable. The diffuse illumination component could then be added to the indices.

Obtaining an adequate number of precisely timed and georeferenced sunlight availability field observations in various stand density and morphology conditions is a prerequisite for evaluating and enhancing the methodologies described but also a major challenge. In addition to logistical cost, illumination conditions often change too rapidly for a human observing a selected number of points. Small ground sunspots generated by sun rays propagating through crowns flicker substantially even with the lightest wind. The point observations used in this study are better suited to quantifying direct sunlight illumination where there is a distinct boundary between sunlit and shadowed areas. Relying on quantum sensors for an instantaneous measurement would likely underestimate direct illumination since the instruments are designed for operation during overcast conditions only. Alternative data collections strategies would hence need to be devised for measuring direct and diffuse illumination conditions simultaneously.

4. Conclusions

This study uses LiDAR data-derived representations of tree crowns and terrain in voxel space and ray tracing to estimate direct sunlight illumination. The effect of voxel resolution is investigated using simulated scenes, also in voxel space. Suggestions on how voxel resolution conducive to unbiased estimation of illumination conditions can be calculated are offered. Remarkable agreement between field measurements of sunlight availability and corresponding LiDAR-data based estimates was observed. Distributed estimates of light transmittance thought canopy or light availability in diffuse form, although not yet implemented in voxel space, are likely attainable and will be investigated in future research. Since the investigation was conducted in low to medium canopy cover conditions and gentle terrain, additional experimentation would be required to determine the approach's performance in close-canopy forests or in the presence of steep slopes.

References

Amanatides, J., and Woo, A. 1987. A fast voxel traversal algorithm for ray tracing. In G. Marechal (Ed.). *Proceeding of EUROGRAPH-ICS'87*, North-Holland, Elsevier Science Publishers: 3-9.

Bellow, J.G., and Nair, P.K.R. 2003. Comparing common methods for assessing understory light availability in shaded-perennial agroforestry systems. *Agricultural and Forest Meteorology*, 114, 197-211.

Burrough, P.A. and McDonell, R.A., 1998. *Principles of Geographical Information Systems*, Oxford University Press, New York, p. 190.

Brunner, A. 1998. A light model for spatially explicit forest stand models. *Forest Ecology and Management*, 107, 19-46.

Chen, Y.D., Carsel, R.F., McCutcheon, S.C., and Nutter, W.L. 1998. Stream temperature simulation of forested riparian areas: I. Watershed-scale model development. *Journal of Environmental Engineering*, 124(4), 304-315.

Comeau, P.G., Braumandl, T.F., and Xie, C.Y. 1993. Effects of overtopping vegetation on light availability and growth of Englemann spruce (*Picea engelmannii*) seedlings. *Canadian Journal of Forest Research*, 23, 2044-2048.

MacFarlane, D.W., Green, E.J., Brunner, A., and Amateis, R.L. 2003.Modeling loblolly pine canopy dynamics for a light capture model, *Forest Ecology and Management*, 173(1–3), 145–168.

Nicotra, A.B., Chazdon, R.L., and Iriarte, S.V.B. 1999. Spatial heterogeneity of light and woody seedling regeneration in tropical we t forests. *Ecology*, 80(6), 1908-1926.

Parendes, L.A., and Jones, J.A. 2000. Role of light availability and dispersal in exotic plant invastion along roads and streasm in the H. J. Andrews Experimental Forest, Oregon. *Conservation Ecology*, 14(1), 64-75.

Parent, S., and Messier, C. 1996. A simple and efficient method to estimate microsite light availability under a forest canopy, *Canadian Journal of Forest Research*, 26(1), 151–154.

Shaw, J.D. 2009. Using FIA data in the Forest Vegetation Simulator. In: W. McWilliams, G. Moisen, R. Czaplewski (Eds). *Forest Inventory and Analysis (FIA) Symposium* 2008; October 21-23, 2008; Park City, UT. Proc. RMRS-P-56CD. Fort Collins, CO: U.S. Department of Agriculture, Forest Service, Rocky Mountain Research Station. 16 p.

Strauss, D.J. 1975. A model for clustering. *Biometrika*, 63, 467–475.

Reda, I., and Andreas, A. 2008. Solar Position Algorithm for Solar Radiation Applications. Technical Report NREL/TP-560-34302, National Renewable Energy Laboratory, Golden, Colorado, 56 pp.